Supplementary files

Title: Smart Hydrogel-based DVDMS/bFGF Nanohybrids for Antibacterial Phototherapy with Multiple Damaging-sites and Accelerated Wound Healing

Authors: Bingjie Mai[1], Mengqi Jia[1], Shupei Liu[1], Zonghai Sheng[2], Min Li[1], Yiru Gao[1], Xiaobing Wang[1], Quanhong Liu[1]*, Pan Wang[1]*

Affiliation:

Key Laboratory of Medicinal Resources and Natural Pharmaceutical Chemistry, Ministry of Education, National Engineering Laboratory for Resource Developing of Endangered Chinese Crude Drugs in Northwest of China, College of Life Sciences, Shaanxi Normal University, Xi'an 710119, Shaanxi, China

[2]Paul C. Lauterbur Research Center for Biomedical Imaging, Institute of Biomedical and Health Engineering, Shenzhen Institutes of Advanced Technology, Chinese Academy of Sciences, Shenzhen 518055, China

Corresponding author: Pan Wang & Quanhong Liu

E-mail: Pan Wang, wangpan@snnu.edu.cn; Quanhong Liu, lshaof@snnu.edu.cn

Telephone: + 86-29-8531 0275

Materials and methods

Characterization of PLGA-bFGF nanoparticles

PLGA-bFGF nanoparticles (PLGA-bFGF NPs) were prepared by the double emulsion-solvent evaporation method. Briefly, bFGF and bovine serum albumin (BSA) solutions were poured into PLGA dichloromethane. The primary emulsion was generated by a high-speed homogenizer (FJ200-SH, Shanghai suoying instruments co., LTD). Afterwards, the resultant emulsion was added to PVA solution and homogenized to obtain the multiple emulsion, and then the emulsion droplets were solidified at room temperature. The NPs were collected by centrifugation and obtained after freeze-drying. The morphology of the NPs was observed using SEM (SU8220, HITACHI, Japan). The Zeta potential was determined by Delsa Nano C Size/Zeta Potential Analysis Instrument (Beckman Instruments, German). The FT-IR spectra of PLGA-BSA, BSA and PLGA were recorded in the range of 400-4000 cm^{-1} using a Perkin Elmer Frontier infrared spectrometer. Stability studies were obtained by detecting the size of PLGA-bFGF stored in PBS, Feta calf serum (FBS) and DMEM culture medium (DMEM CM). The PLGA-NPs and CSDP hydrogels were placed in 2 ml of PBS (pH 7.4 and pH 6.8) and incubated with shaking (100 rpm) at 37 °C for 18 days. At designated time point, the supernatant was collected and equal amount of fresh medium was added to each sample. Adopting the ELISA Assay Kit to detect the bFGF concentration in releasing media.

Biocompatibility evaluation of the CSDP

Hemolytic activity was determined by incubating suspensions of human red blood cells with CSDP. Red blood cells were rinsed several times in PBS by centrifugation for 3 min at 3000 g until the OD of the supernatant reached the OD of the control. Red blood cells were counted by a hemocytometer and adjusted to $7.7 \times 10^6 \pm 0.3 \times 10^6$ cells/ml. Red blood cells were then incubated at room temperature for 1 h in 2% Triton X-100 (Positive control), in PBS (Control), or with different hydrogels. The samples were then centrifuged at 10000 g for 5 min, the supernatant was separated from the pellet, and its absorbance measured at 570 nm. The relative optical density compared

to that of the suspension treated with PBS was defined as the percentage of hemolysis. The cytotoxicity was measured by employing a direct contact test between hydrogels and NIH3T3 cells. NIH3T3 cells were seeded in 96-well plate at a density of 10000 cells/well. After cultured for 24 h, the hydrogels were introduced into the wells. The cell proliferation under the hydrogel was evaluated by CCK 8 Kit and calcein AM/PI staining after 12 h and 24 h.

The Balb/c mouse back skin was shaved 24 h before the experiment to allow for full recovery from possible disturbance to the stratum corneum by the shaving process. The CSDP was administrated onto the shaved area. The mice administrated with PBS served as a control group. After 14 days treatment, all the mice were sacrificed, and the treated areas were collected for histological examination. To fix the tissue, the skin samples were immersed into 10% formalin for 18 h and then embedded in paraffin. H&E staining and TUNEL assay were used to evaluate the cellular morphology change and apoptosis, respectively. Tissue slices were imaged with fluorescence microscopy.

Evaluation of the antibacterial activity of free DVDMS-PACT and antibiotic

S. aureus and MDR-*S. aureus* suspensions (10^8 CFU/ml) were respectively added to free DVDMS (2, 5, 10 μg/ml) prepared in a 24-well flat-bottomed plate, and incubated for 75 min at 37 °C. After irradiating with different laser doses (10, 20, 30 J/cm^2), CFUs were counted. For comparison, suspensions of bacteria were parallelly incubated with different concentration of antibiotics-Levofloxacin, Ciprofloxacin and Clindamycin for 75 min at 37 °C, CFUs were counted, respectively.

Effect of PLGA-bFGF on wound healing

To verify the efficacy of PLGA-bFGF NPs in promoting wound healing, 0.785 cm^2 circle full-thickness wound in skin was made on the dorsal surface of each mouse. Subsequently, PLGA-bFGF NPs were applied to each of the following days to observe the healing of the skin. For evaluation of skin regeneration in wound area, the regenerated skin collected on 21 day was used to perform H&E and Masson trichrome stain. Histopathological changes were observed using microscopy. Subsequently, the regenerated skins from the wound site were also excised at 7, 14 and 21 day for immunofluorescence staining. The fixed and frozen sections were stained with bFGF

antibody (Abcam). FITC-conjugated goat anti-rabbit IgG (Abcam) was used as the secondary antibody to reveal bFGF expression. The nuclei were counterstained with DAPI mounting solution. Slides were observed under a fluorescence microscope.

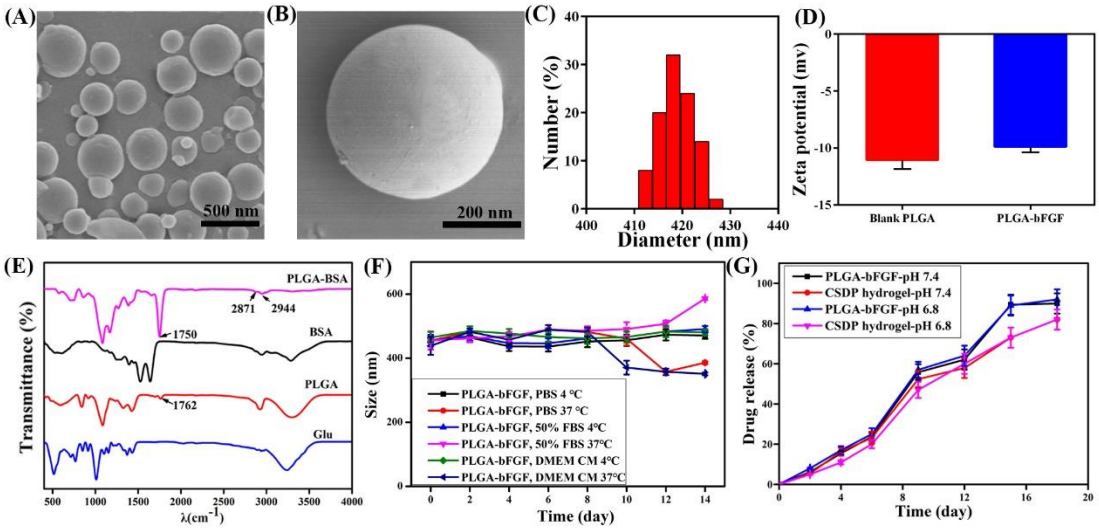

Figure S1. Characterization of PLGA-bFGF nanoparticles. (A) SEM image of PLGA-bFGF. Scale bar=500 nm. (B) High magnification image of PLGA-bFGF. Scale bar= 200 nm. (C) DLS particle size distribution of PLGA-bFGF. (D) Zeta potential of Blank PLGA and PLGA-bFGF. (E) FT-IR spectra of Glu, PLGA, BSA and PLGA-BSA. (F) Changes in diameters of PLGA-bFGF after storage at 4 °C and 37 °C for different times in the presence of PBS, FBS and DMEM CM. (G) *In vitro* release profiles of the PLGA-bFGF and CSDP hydrogel at pH values of 7.4 and 6.8. Data are expressed as mean ± SD of three independent experiments.

(A)

Sample	CMCS (g)	SA (g)	EDC (mg)	NHS (mg)	EDC/NHS (mmol/mmol)	Gelation Time (25 ℃)	Product
CSDP 0.75	0.25	0.25	72	44.25	0.75/0.75	>300 s	Solution
CSDP 1.00	0.25	0.25	96	59	1/1	~90 s	Gel
CSDP 1.25	0.25	0.25	120	73.75	1.25/1.25	~55 s	Gel
CSDP 1.50	0.25	0.25	144	88.5	1.5/1.5	~30 s	Gel

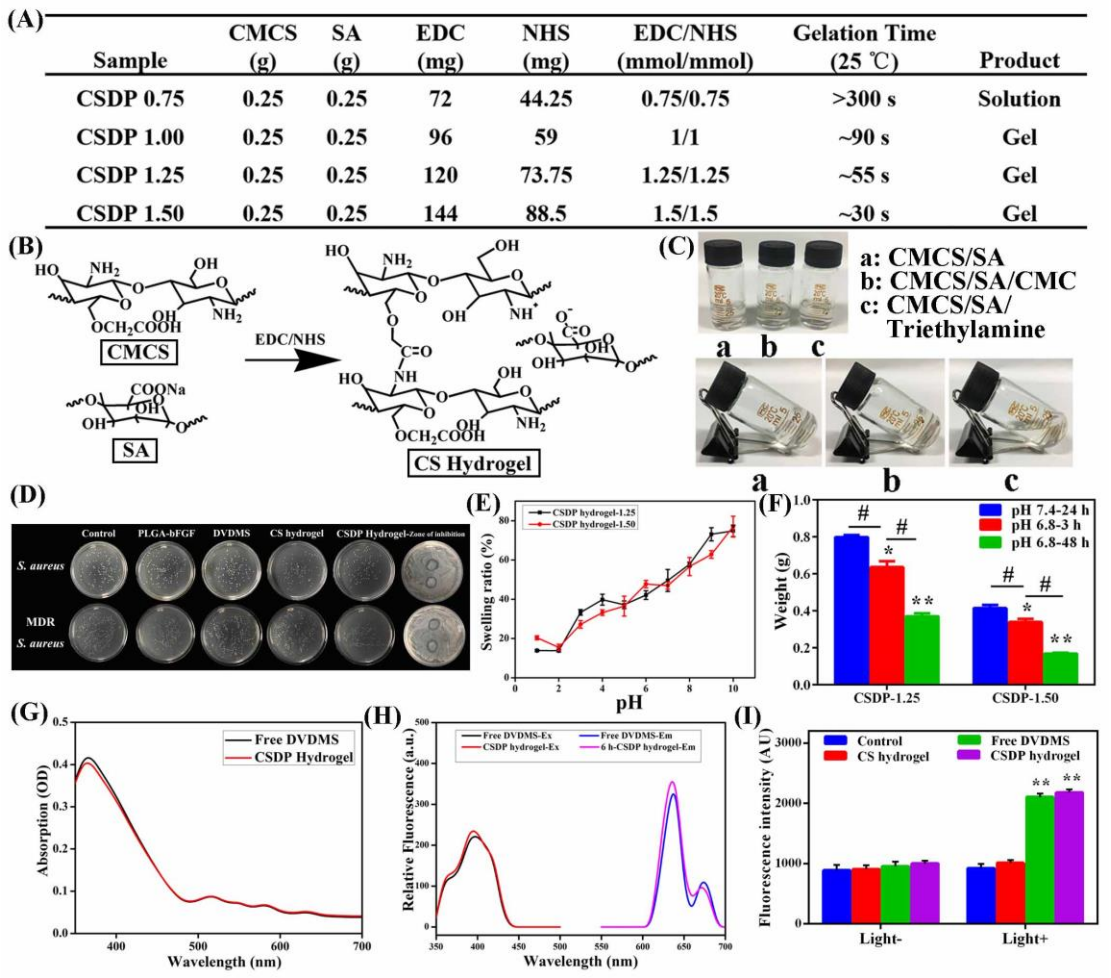

Figure S2. Characterization of CSDP hydrogel. (A) Parameters and gelation time of hydrogel samples. (B) Synthesis scheme of CS hydrogel. (C) Identification of ionic bonds in the synthetic reactions. a) CMCS-SA, b) CMCS-SA-CMC, c) CMCS-SA-Triethylamine. (D) Bacteria counts of *S. aureus*/MDR-*S. aureus* with PLGA-bFGF, CS hydrogel and CSDP hydrogel treatment. Right inset: photographs shows the inhibition zone of CSDP hydrogel against *S. aureus*/MDR-*S. aureus*. (E) Equilibrium swelling ratio of hydrogels after swelling for 24 h in different PBS (pH 1-10). (F) Effects of pH change and incubation time on the swelling quality of CSDP hydrogel. Absorption spectra (G) and Fluorescence spectra (H) of Free DVDMS and DVDMS released from CSDP hydrogel. (I) Singlet oxygen production of free DVDMS and DVDMS released from CSDP hydrogel. Data are expressed as mean ± SD of three independent experiments, *p<0.05, *p<0.01 *versus* Control, #p<0.05 between groups.

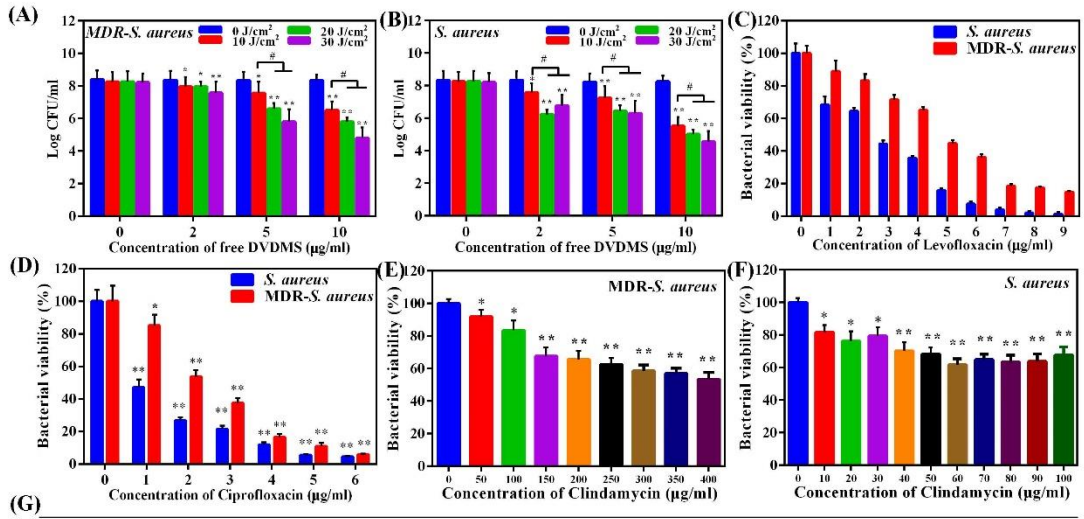

(G)

	0 J/cm²				10 J/cm²				20 J/cm²				30 J/cm²			
Strains	*S. aureus*		*MDR-S. aureus*		*S. aureus*		*MDR-S. aureus*		*S. aureus*		*MDR-S. aureus*		*S. aureus*		*MDR-S. aureus*	
Drugs	free DVDMS	CSDP hydrogel	free DVDMS	CSDP hydrogel	free DVDMS	CSDP hydrogel	free DVDMS	CSDP hydrogel	free DVDMS	CSDP hydrogel	free DVDMS	CSDP hydrogel	free DVDMS	CSDP hydrogel	free DVDMS	CSDP hydrogel
0 μg/ml	100	100	100	100	81.2785	81.2832	72.6531	72.6523	83.105	83.1152	74.2857	74.2952	73.9726	73.9731	66.1224	66.1234
2 μg/ml	99.5434	99.5423	95.5102	95.5152	16.9863	10.6849	38.0816	30.2463	0.7763	0.2452	38.0816	24.0432	0.9315	0.0269	15.5102	7.8012
5 μg/ml	81.2785	77.6256	88.9796	89.3913	7.9452	0.5023	14.8163	9.3552	1.2877	0.0129	1.6245	0.5142	0.9315	0.0009	0.2575	0.1289
10 μg/ml	77.6256	81.2785	89.3878	89.3914	0.1479	0.1479	1.2898	0.5142	0.0466	0.0047	0.2576	0.0816	0.0166	0.0005	0.0276	0.0041

(H)

Levofloxacin											
	Concentration (μg/ml)	0	1	2	3	4	5	6	7	8	9
S. aureus	Bacterial viability (%)	100	68.31	64.44	43.32	35.59	15.72	7.48	3.87	1.94	1.17
MDR-S. aureus	Bacterial viability (%)	100	88.81	83.17	71.45	65.03	44.69	36.03	18.51	17.31	14.79

(I)

Ciprofloxacin							
	Concentration (μg/ml)	0	1	2	3	4	5	6
S. aureus	Bacterial viability (%)	100	47.12	26.75	21.56	11.94	5.51	4.59
MDR-S. aureus	Bacterial viability (%)	100	85.03	53.63	37.52	16.52	10.97	5.81

(J)

Clindamycin-MDR *S. aureus*											
Concentration (μg/ml)	0	10	20	30	40	50	60	70	80	90	100
Bacterial viability (%)	100	81.65	76.22	79.35	70.24	68.32	61.79	64.92	63.41	63.83	67.75

(K)

Clindamycin- *S. aureus*									
Concentration (μg/ml)	0	50	100	150	200	250	300	350	400
Bacterial viability (%)	100	91.81	83.46	67.58	65.56	62.56	58.52	57.01	53.41

Figure S3. Antibacterial activity of different treatment for *S. aureus*/MDR-*S. aureus*. CFU analysis of MDR-*S. aureus* (A) and *S. aureus* (B) after free DVDMS-PACT treatment. (C) Bacterial viability of levofloxacin for *S. aureus*/MDR-*S. aureus*. (D) Bacterial viability of ciprofloxacin for *S. aureus*/MDR-*S. aureus*. Bacterial viability of clindamycin for MDR-*S. aureus* (E) and *S. aureus* (F). (G) Bacterial viability of free DVDMS-PACT and CSDP Hydrogel-PACT for *S. aureus*/MDR-*S. aureus*. (H) Bacterial survival percentage of (C). (I) Bacterial survival percentage of (D). (J) Bacterial survival percentage of (E). (K) Bacterial survival percentage of (F). Data are expressed as mean ± SD of four independent experiments, *p<0.05, *p<0.01 *versus* Control, #p<0.05 between groups.

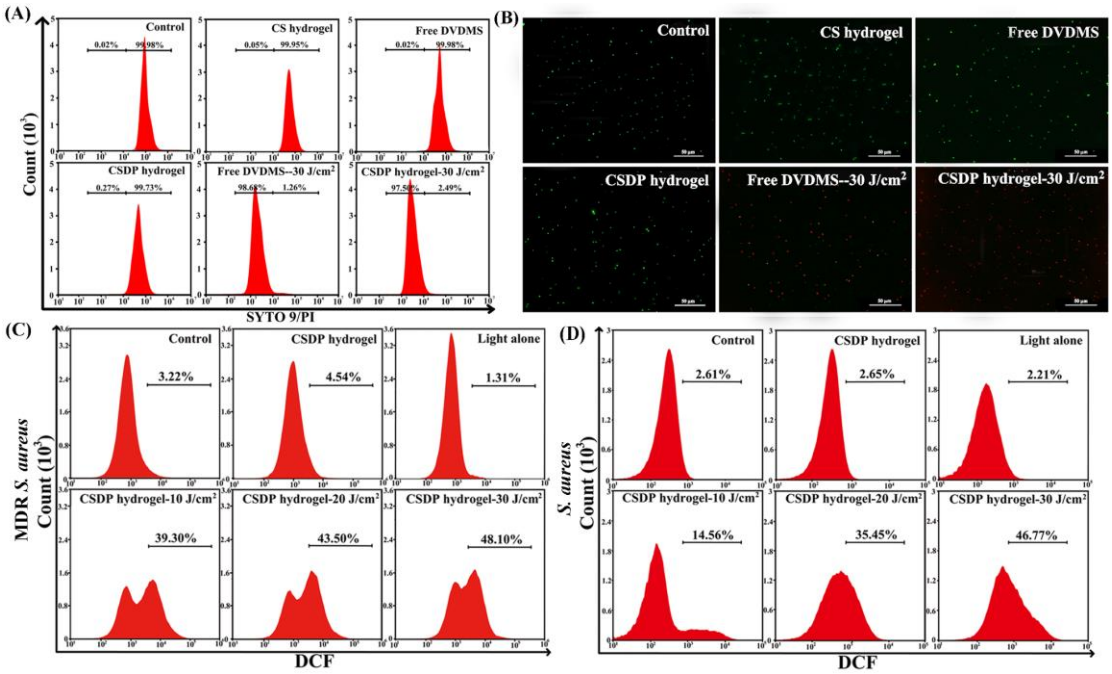

Figure S4. Antibacterial activity of CSDP-PACT for *S. aureus*. Flow cytometry (A) and fluorescence microscopy (B) combined with SYTO 9/PI staining to illustrate bacterial viability. Intracellular ROS generation of MDR-*S. aureus* (C) and *S. aureus* (D) detected by DCFH-DA as measured by flow cytometry. Data are expressed as mean ±SD of three independent experiments, Scale bar=50 μm.

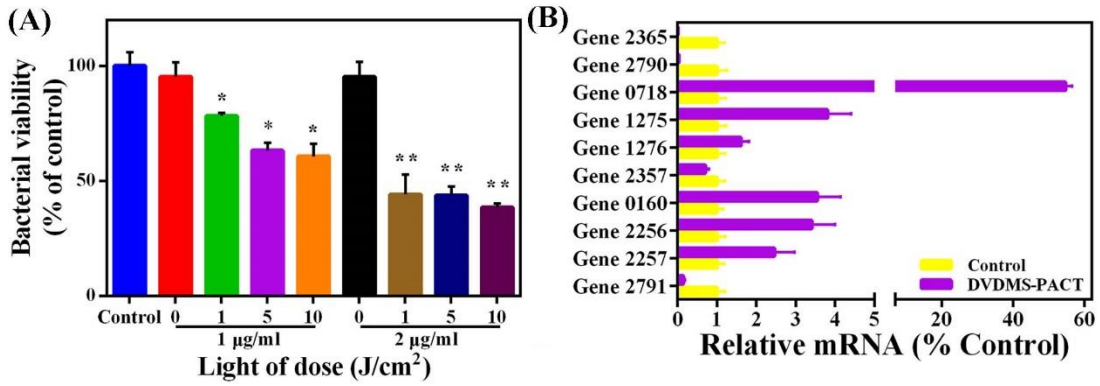

Figure S5. (A) Effect of DVDMS-PACT on MDR-*S. aureus*. (B) Selected MDR-*S. aureus* genes that displayed altered expression after DVDMS-PACT treatment as determined by RT-PCR. Data are expressed as mean ± SD of three independent experiments, *p<0.05, **p<0.01 *versus* Control.

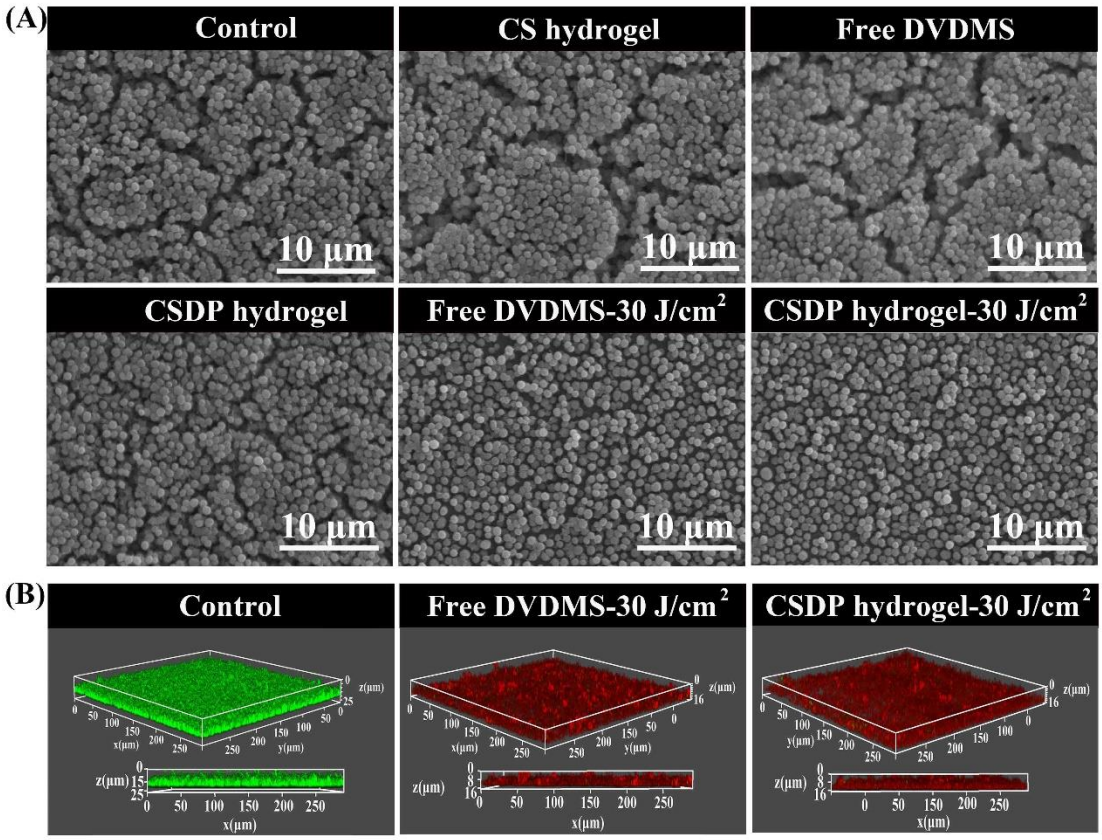

Figure S6. *S. aureus* biofilms disrupted by CSDP-PACT. (A) SEM images of *S. aureus* biofilms with different treatment. Scale bar=10 μm. (B) 3D confocal images of *S. aureus* biofilms with different treatment.

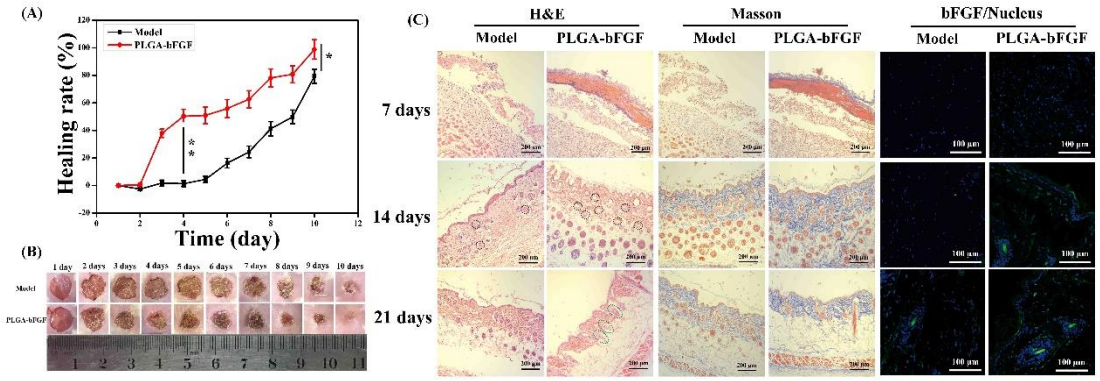

Figure S7. Effect of PLGA-bFGF on wound healing. Skin wound healing rate (%) (A) and representative images of wounds (B) in the different treatment groups. (C) Representative photographs of skin wound tissues on day 7, day 14 and day 21 after H&E, Masson and bFGF (green) immunofluorescence. Data are expressed as mean ± SD of four independent experiments, *p<0.05, **p<0.01 *versus* Model.

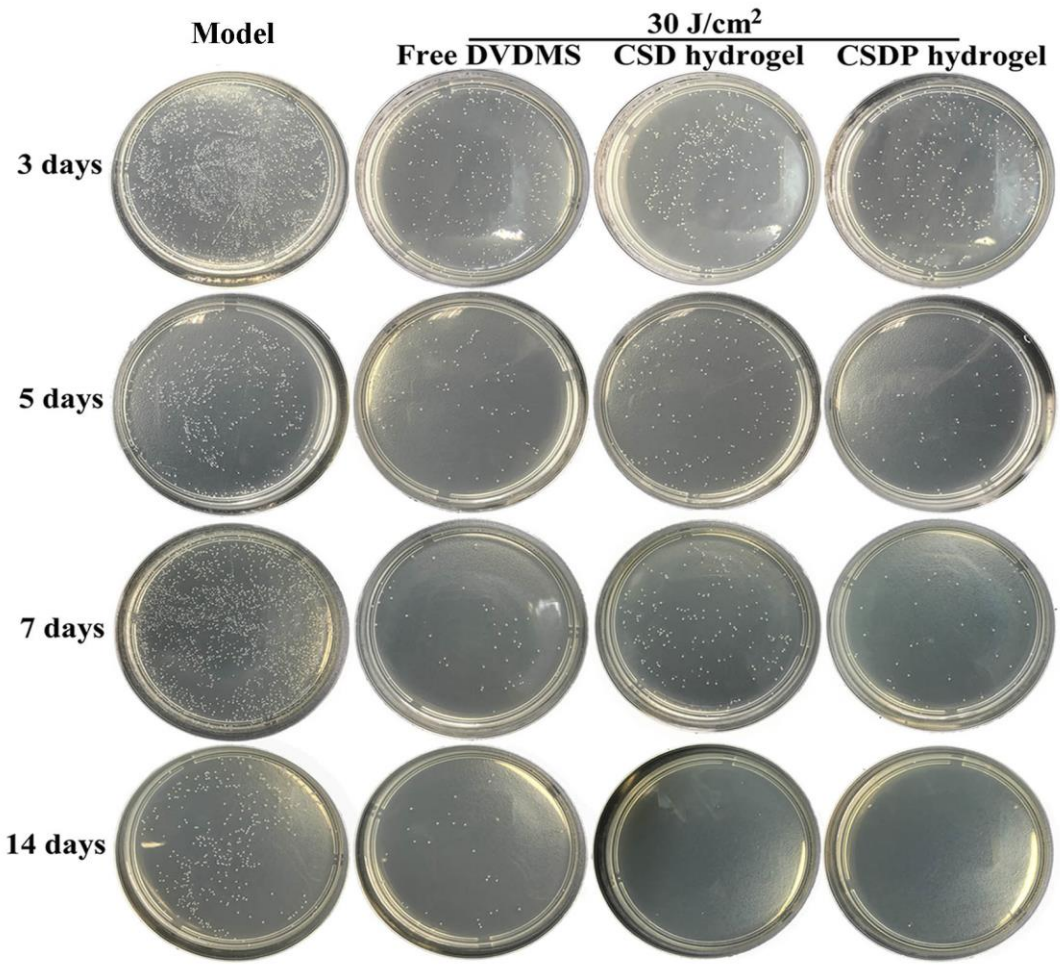

Figure S8. Representative bacterial colonies with different treatment.

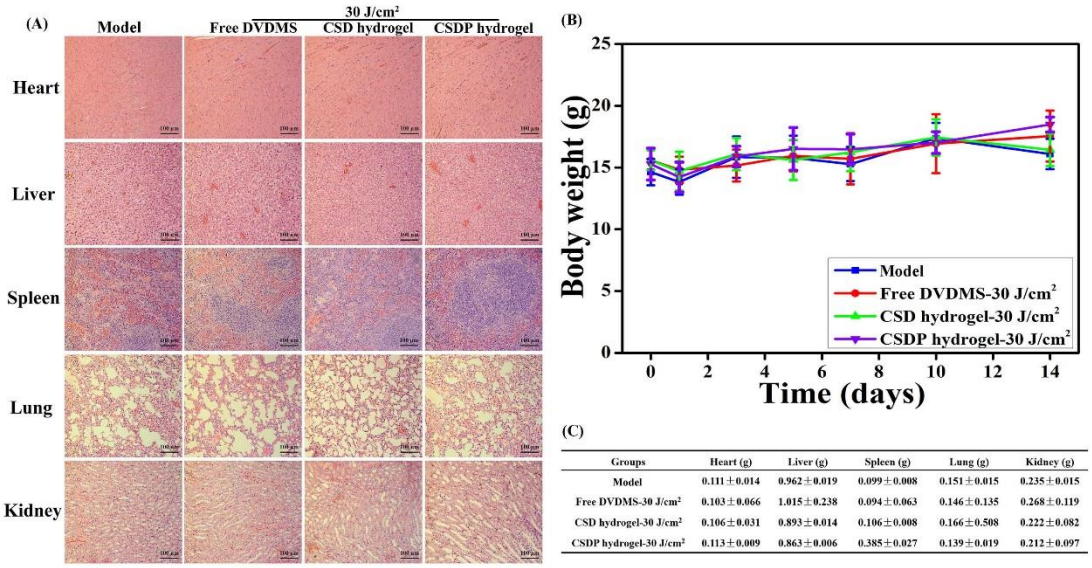

(C)

Groups	Heart (g)	Liver (g)	Spleen (g)	Lung (g)	Kidney (g)
Model	0.111±0.014	0.962±0.019	0.099±0.008	0.151±0.015	0.235±0.015
Free DVDMS-30 J/cm²	0.103±0.066	1.015±0.238	0.094±0.063	0.146±0.135	0.268±0.119
CSD hydrogel-30 J/cm²	0.106±0.031	0.893±0.014	0.106±0.008	0.166±0.508	0.222±0.082
CSDP hydrogel-30 J/cm²	0.113±0.009	0.863±0.006	0.385±0.027	0.139±0.019	0.212±0.097

Figure S9. Evaluation of side effects using CSDP-PACT. (A) H&E staining of heart, liver, spleen, lung, and kidney slices after 21-days treatment for the different groups. Scale bar=100 μm. (B) Body weight changes after different treatments. (C) Weights of major organs in the mice. Data shown as means ± SD from four mice in each group.

Table S1: Differential genes in the KEGG pathway.

KEGG	Gene_id	readcount_PACT	readcount_Control	log2FoldChange	pval	padj	GeneName	Descrition
	gene2791	127.8910872	1419.339624	-3.4722	2.37E-23	6.05E-20	SAOUHSC_02969	arginine deiminase
	gene2790	193.0561906	1033.725288	-2.4208	1.11E-13	2.84E-11	SAOUHSC_02968	ornithine carbamoyl transferase
	gene2788	618.9552296	1908.319759	-1.6244	1.20E-07	1.17E-05	SAOUHSC_02965	carbamatekinase
	gene2019	21.82074323	99.64348862	-2.1911	1.26E-06	9.18E-05	SAOUHSC_02134	nitricoxide synthase oxygenase subunit
	gene2332	132.8860901	420.3138234	-1.6613	6.11E-06	0.00034612	SAOUHSC_02468	acetolactate synthase
	gene1275	75.51770936	19.75005169	1.935	5.93E-05	0.0021923	SAOUHSC_01366	anthranilate synthase componentI
	gene403	1613.484711	653.8092783	1.3032	7.84E-05	0.0027025	gltD	glutamate synthase subunitbeta
Amino acids	gene2020	17.16669899	59.90062393	-1.803	0.00014905	0.0044212	SAOUHSC_02135	hypothetical protein
	gene2417	513.9483605	1207.210438	-1.232	0.00016979	0.0048109	ureC	urease subunitalpha
	gene1766	3949.449721	2090.079793	0.91809	0.0013662	0.022059	SAOUHSC_01901	putativetranslaldolase
	gene1276	36.23381815	11.303976	1.6805	0.0014647	0.02267	SAOUHSC_01367	anthranilate synthase component II
	gene2674	19.59400853	62.04700106	-1.6629	0.0014732	0.02267	SAOUHSC_02840	L-serinedehydrataseiron-sulfur-dependentsubunitbeta
	gene402	4186.343445	1950.873409	1.1016	0.0015223	0.023115	SAOUHSC_00435	glutamatesynthaselargesubunit
	gene1277	85.19393066	31.64775602	1.4286	0.0029506	0.037477	trpD	anthranilate phosphoribosyl transferase
	gene745	3715.005868	6899.643548	-0.89316	0.00394	0.045895	tpiA	triosephosphateisomerase
	gene2357	212.3481249	1140.073798	-2.4246	2.85E-12	5.19E-10	rpsE	30S ribosomal protein S5
	gene2361	11.00861108	58.72674801	-2.4154	1.51E-05	0.0007536	rpsN	30S ribosomal proteinS14
Ribosome	gene2356	8.077682908	50.2580743	-2.6373	1.61E-05	0.00079053	rpmD	50S ribosomal proteinL30
	gene2359	176.0027938	1359.335493	-2.9492	9.96E-05	0.0033418	rplF	50S ribosomal proteinL6
	gene2369	123.446904	1035.421576	-3.0683	0.0003053	0.0072113	rplV	50S ribosomal proteinL22
Peptidoglycan biosynthesis	gene1905	1996.235297	560.1942698	1.8333	1.24E-07	1.17E-05	SAOUHSC_02012	glycosyl transferase
	gene1076	145.026976	343.6440949	-1.2446	0.00028194	0.0068499	murD	UDP-N-acetylmuramoyl-L-alanyl-D-glutamatesynthetase
Pentose phosphate pathway	gene2247	1475.274422	564.288045	1.3865	3.57E-05	0.001517	SAOUHSC_02379	2-deoxyribose-5-phosphatealdolase
	gene1766	3949.449721	2090.079793	0.91809	0.0013662	0.022059	SAOUHSC_01901	putativetranslaldolase

Table S2. Primers used in real-time RT-PCR with SYBR green probes.

Target gene	Primer	Sequence (5'-3')
16S rRNA	16S rRNA for	CGTGCTACAATGGACAATACAAA
	16S rRNA rev	ATCTACGATTACTAGCGATTCCA
Gene 2365-rpsQ	Gene 2365 for	TCTGCAAGGTCGCGTTGTTAGC
	Gene 2365 rev	CTTGGACAGCGGACGGCATTC
Gene 2790-SAOUHSC_02968	Gene 2790 for	GTGCAGCGTTTACAGTTGCG
	Gene 2790 rev	CCACACCGGTACACCAGAGA
Gene 0718-secA	Gene 0718 for	CGTTCAGTTACTCGGCGGTATGG
	Gene 0718 rev	TTCAGGTAAGCAGGCAGCGTTG
Gene 1275-SAOUHSC_01366	Gene 1275 for	TCAACGTGGTGAGACGACAC
	Gene 1275 rev	AGCATACGATGTTCGCTGCAT
Gene 1276-SAOUHSC_01367	Gene 1276 for	TGGTCCAGGGCATCCATTAGA
	Gene 1276 rev	CGTGCATAACCTTGTCGCCT
Gene 2357-rpsE	Gene 2357 for	CGTGAAGTTCCAGCAGCGATCC
	Gene 2357 rev	ATTGCACCACCGGCGATGATAC
Gene 0160-SAOUHSC_00173	Gene 0160 for	AGGACCTGCTGCTGATTTTGA
	Gene 0160 rev	AGGTTCAGCATTGTGTCCTTCA
Gene 2256-SAOUHSC_02388	Gene 2256 for	TCAGTCAGCGAAGCAAGTGTTGG
	Gene 2256 rev	AGGATGATTCGCGTGATGTATGGC
Gene 2257-SAOUHSC_02389	Gene 2257 for	GGCGGTCTCCTTGCTAACAG
	Gene 2257 rev	TGCGACAAGTGCAACACCTA
Gene 2791-SAOUHSC_02969	Gene 2791 for	GACCAGGCGTTGTAGTGACTTACG
	Gene 2791 rev	TCCACGTACCAACTCGCTACCAG

Table S3. Selected MDR-*S. aureus* genes that displayed altered expression after DVDMS-PACT treatment as determined by microarray analysis and RT-PCR.

Gene	Description	Fold change ± SD	
		RT-PCR	RNA-seq
Gene 2365 rpsQ	30S ribosomal protein S17	-6.60	-2.6873
Gene 2790 SAOUHSC_02968	Ornithine carbamoyl transferase	-4.94	-2.4208
Gene 0718 secA	Preprotein translocase subunit SecA	5.77	1.4466
Gene 1275 SAOUHSC_01366	Anthranilate synthase component I	1.93	1.935
Gene 1276 SAOUHSC_01367	Anthranilate synthase component II	0.69	1.6805
Gene 2357 rpsE	30 S ribosomal protein S5	-0.50	-2.4246
Gene 0160 SAOUHSC_00173	azoreductase	1.83	2.4427
Gene 2256 SAOUHSC_02388	Hypothetical protein	1.77	3.6516
Gene 2257 SAOUHSC_02389	Cation efflux family protein	1.30	3.4137
Gene 2791 SAOUHSC_02969	Arginine deiminase	-2.81	-3.4722